HIGH-RESOLUTION GEOLOGICAL SURVEY BY HIGH FREQUENCY SEISMIC WAVE

JUNICHI SAKAKIBARA [i], YOSHITO YAMAUCHI [ii] and KOJI KAYUKAWA [iii]

ABSTRACT

A high-resolution geological survey by high frequency seismic wave has been developed. This method is designed to transmit a pseudo random binary sequence wave of desired frequency. We can measure an accurate geological structure between wells separated by a long distance. This new method was conducted to locate a firm silt layer accurately for a pile foundation work of a multistory car park in Chubu International Airport. Accurately visualized images of the firm silt layer enabled us to design exact lengths of the pile foundation. The actual cost of the foundation work was compared with the cost estimated by designing based on only boring logs and it was found that 40 % of cost of the foundation work was saved by this new method.

Key Words : Seismic wave, High Frequency, Geological Survey, Pseudo Random Binary Sequence (**IGC**: E4)

1 INTRODUCTION

Exact understanding of a ground structure can bring accurate and effective design including foundation design, soil improvement, tunnel construction while reducing cost and work period as well as ensuring safety before and after the construction. Usually, we use boring log for foundation designing and sometimes encounter "shortage or excess of pile length" because we have to estimate the ground structure between boreholes as shown in Fig.1. A two-dimensional visualization of the ground structure such as seismic tomography can keep us away from these problems because we can obtain the continuous ground structure image without estimating. But the previous seismic tomography has not been standard method yet for the foundation designing because of two reasons, low resolution and difficulty of interpretation.

First, a frequency is one of the most influent factors of the resolution. The resolution ϕ is defined by the wavelength λ, the frequency f and the velocity of the seismic wave as shown in equation (1) to (3) (Sakakibara et al, 2009),

$$\phi = \frac{\lambda}{2} \tag{1}$$

$$\lambda = \frac{V}{f} \tag{2}$$

$$\phi = \frac{V}{2f}. \tag{3}$$

For example, the frequency of the conventional seismic tomography is typically lower than 200Hz. If the velocity of the seismic wave in the ground is 2,000m/s, the resolution can be calculated 5m from equation (3), however 5m is not enough accurate to design the pile length of the pile foundation.

Second, sometimes it is difficult to understand the result of the conventional seismic tomography because the conventional seismic tomography provides the only velocity image. The velocity is only square root of bulk modulus K to density ρ ratio as shown in equation (4),

$$V = \sqrt{\frac{K}{\rho}}. \tag{4}$$

For example, the velocity in the sand is generally faster than the velocity in the clay but sometimes the velocity in the loose sand is not faster than the velocity in the compacted clay. In this case, we may misunderstand the compacted clay as the loose sand.

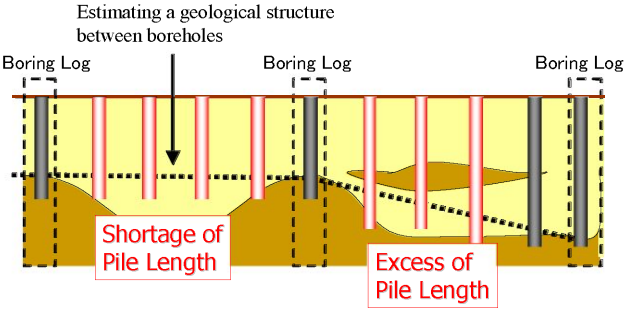

Fig. 1. Problems encountered while pile foundation work

[i] Group leader of geo-acoustics group, JFE Civil Engineering & Construction Corporation, 2-17-4, Kuramae, Taitoku, Tokyo, 111-0051, Japan.
[ii] Head Researcher, Geo-Research Institute- Kyushu office, 2-5-1 Akebono, Sawara-ku, Fukuoka 814-0004, Japan
[iii] PE, Geo-Research Institute, 1-8-4, Yushima, Bumkyoku, Tokyo, 113-0034, Japan
Manuscript was received for review on September 15, 2009.

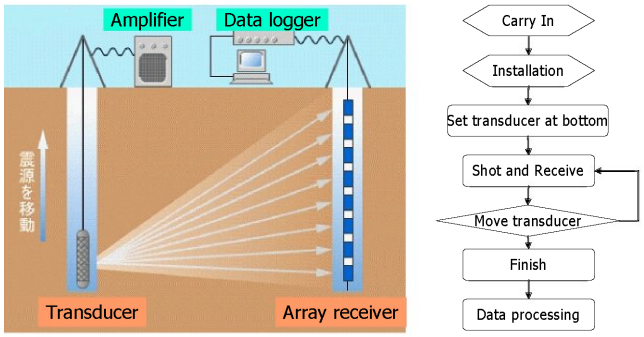

Fig. 2. Schematic image of data acquisition system

Fig. 3. Photos of the transducer (left) and the arrayed receiver (right)

Sakakibara et al (2009) have newly developed the high resolution seismic tomography by using the high frequency seismic wave to dissolve these problems. This method is characterized by not only the high resolution and the easy interpretation also a long distance, and a noise proof. In this paper, this new tomography is explained by comparing with the conventional seismic tomography. Then past results are shown and verified its cost advantage. Finally, a new construction flow by using this new tomography is proposed.

2 HIGH FREQUENCY SEISMIC WAVE TOMOGRAPHY

2.1 Data acquisition and processing system

A data acquisition system consists of a transducer, an arrayed receiver, a power amplifier, a data logger and a signal filter as shown in Fig.2, Fig.3 and Table 1. We use the piezo-electric type transducer which is available from 100Hz to 20kHz in frequency. We also use the arrayed receiver which has 24 underwater microphones, which are available from 1Hz to 20kHz in frequency, with 1m spacing. These transducer and receiver are designed to use up to 200m in depth. Measurement boreholes for the transducer and the receiver should be protected by PVC casing pipe which is more than 50mm in inner diameter and filled by water. The transducer should be installed at the bottom of the borehole and moved up by planed interval after shooting and receiving the seismic wave as shown as Fig.2.

A schematic image of the data processing flow is shown in Fig.4. An arrival time and a sound pressure level of the first arrival waves are read from each received waves. The velocity V and an attenuation L are calculated from equation (5) and equation (6),

$$V = \frac{D}{t} \tag{5}$$

$$L = Li + Lt + L_s = A_0 - A - L_d \tag{6}$$

where D, t, A_0, A, L_i, L_t, L_d, L_s are the distance between the transducer and the receiver, the travel

Table 1. Specification of the data acquisition system

item	specification
Transducer	piezo electric type, outer diameter 44mm, length 270mm, weight 4.5kg, available output frequency 100Hz to 20kHz, output 130.6dB(at input voltage 100V, frequency 5kHz)
Receiver	piezo electric type, outer diameter 35mm, array spacing 1m, number of arrays 24, weight 11kg, available frequency band 1Hz to 20kHz, sensitivity -162 dB re 1V/μPa
Power amplifier	output 120V(<20kHz), available frequency band 20Hz to 20kHz, input AC100V, electric power consumption 60W, weight 9kg
Signal filter	output gain 1 to 100 times, number of channel 8ch, band pass filter 200Hz to 60kHz, input DC±12V
Data logger	number of input channel 8ch, input resolution 14bit, weight 7kg

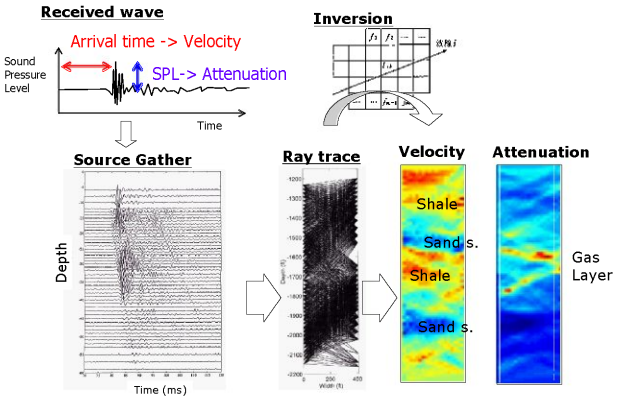

Fig. 4. Schematic image of the data processing flow

time, a sound pressure level of the transmitted wave, the sound pressure level of the received wave, an intrinsic loss, a transparent loss and a scattering loss

respectively (Yamamoto et al, 1994). Then we calculate and output the velocity image and the attenuation image by a ray tracing method and an inversion method (Bergman et al, 1989). Generally speaking, the velocity represents kinds of the ground and a hardness of the ground and the attenuation represents a particle size of the soil and an internal gas or fluid in the ground.

2.2 Pseudo random binary sequence wave

Pseudo random binary sequence (PRBS) wave is one of the pulse compression methods (Cunningham, 1979). As shown in Fig.5, an output wave (transmit wave) is a periodic phase modulated sign wave. The received wave is also the periodic wave which is more complicated than the output wave. A cross correlated wave between the transmit wave and the received wave looks a pulse wave. We can equate the arrival time and the height of the peak of the cross correlated wave to "arrival time" and "amplitude" of a propagated wave in the ground respectively. Using the PRBS wave has three merits, "increasing a signal to noise ratio", "transmitting a single frequency" and "no error in reading wave" as shown in Fig.6.

First, increasing the signal to noise ratio allows us to read the small wave which is attenuated by propagating from a distance and smaller than the background noise. Second, transmitting a single frequency allows us to transmit a desired frequency. Third, no error in reading allows us to conduct the accurate measurement and save our time to do the data processing. It also allows us to do the attenuation tomography. These merits bring us three advantages, "long distance measurement", "high resolution", "easy interpretation from two different images".

2.3 Advantage of the new tomography (1) "long distance and high resolution"

The sound wave is attenuated in proportion to exponential of the frequency as shown in equation (7) and (8),

$$A = \frac{1}{r} A_0 e^{-\alpha r} \qquad (7)$$

$$\alpha = \frac{\pi f}{VQ}, \qquad (8)$$

where r, α, Q, are a propagated distance, a attenuation factor and a quality factor respectively (Yamamoto et al, 1994). Transmitting the high frequency sound wave is difficult because of this reason. As shown in Fig.7, if we use the conventional tomography, the low frequency wave propagates for long distance but it doesn't have the high resolution. On the other hand, the high frequency wave doesn't propagate for long distance but it has the high resolution. If we use the PRBS wave, the high frequency wave propagates for long distance and has the high resolution because the signal to noise ratio is much increased.

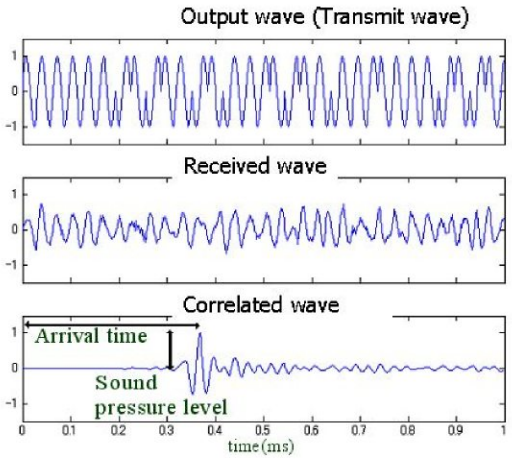

Fig. 5. PRBS wave, transmit wave (upper), received wave (middle), correlated wave (lower)

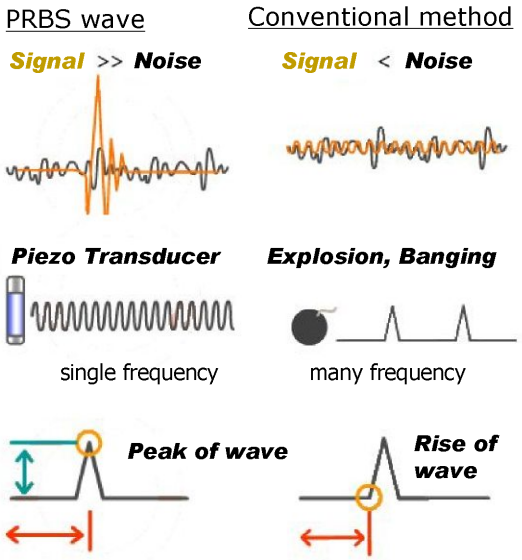

Fig. 6. Merits of PRBS wave, increasing a signal to noise ratio (upper), transmitting a single frequency (middle), no error in reading (lower)

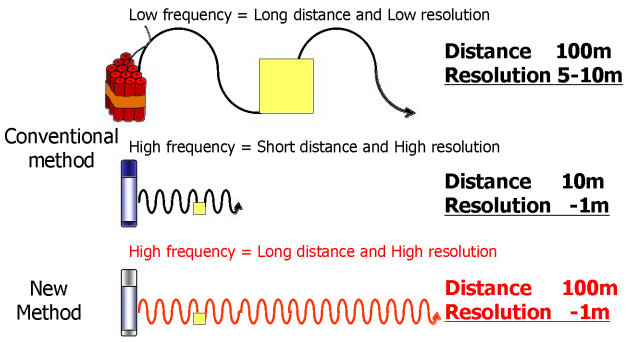

Fig. 7. Comparison with the conventional method from points of view of the propagating distance and the resolution

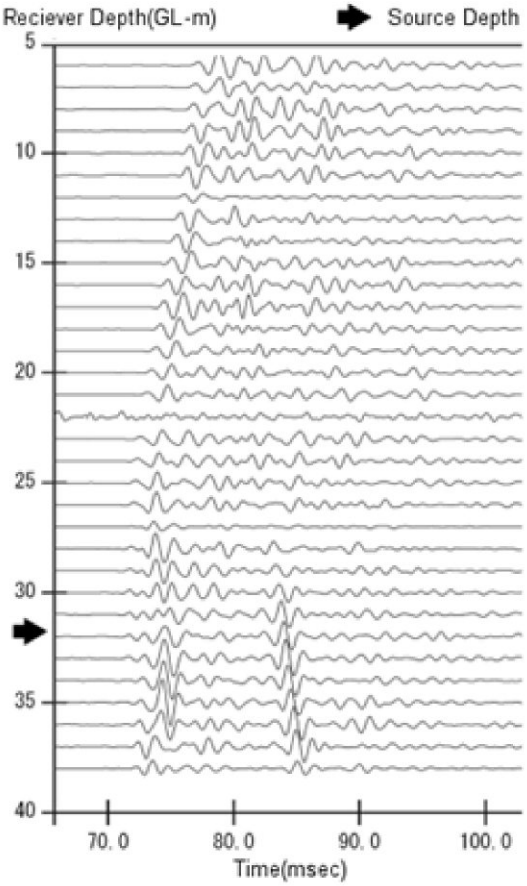

Fig. 8. Source gather of the correlated PRBS wave propagated in sediments of Tokyo Bay, 100m in distance between the transducer and receiver array, 1kHz in frequency.

Fig.8 shows a source gather of the correlated PRBS wave propagated in the sediments of Tokyo bay. The arrival waves look clear though the distance between measurement boreholes was 100m and the frequency was 1kHz. Meanwhile the new tomography can't be used in unsaturated sediments because the higher frequency wave attenuates significantly in the unsaturated sediments.

2.4 Advantage of the new tomography (2) "easy interpretation"

The velocity image shows the ground structure in general but sometimes it is difficult to understand the result of the seismic tomography as we discussed in chapter 1. Using the new tomography, it is easier to understand its results since the new tomography outputs two results, the velocity image and the attenuation image coincidentally. The attenuation image represents the fluid in the porous media or the grain diameter. For example, the attenuation in the sand is higher than the attenuation in the clay because of the difference of the grain diameters. So we can recognize the sand and the

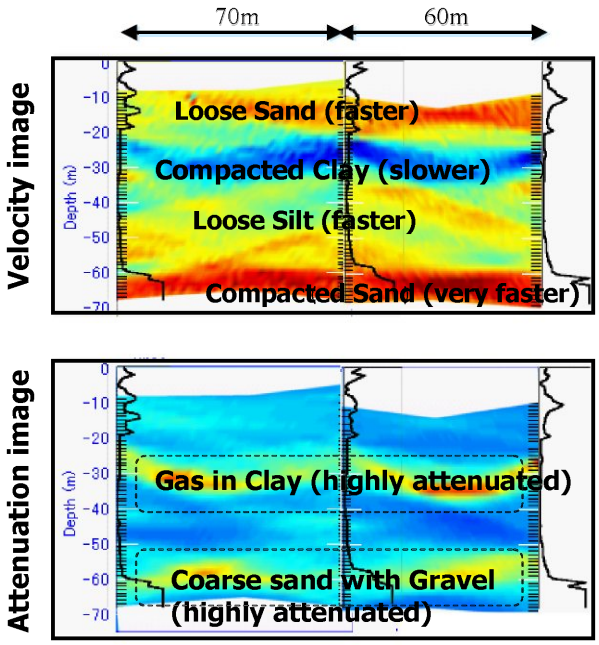

Fig. 9. Experimental results at Tokyo Bay. The velocity image (left) and the attenuation image at 1kHz. The distances between boreholes are 70m and 60m.

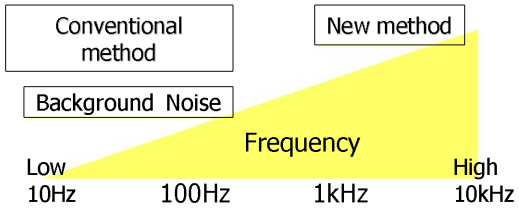

Fig. 10. Comparison of frequency band of the conventional tomography, the new tomography and the background noise

clay even though the velocity in the sand is same as in the clay.

Fig.9 shows the velocity image and the attenuation image of experimental results at Tokyo Bay. The velocity image (upper) shows the sand layers as faster areas (yellow and red color) and the clay layer as slower areas (blue color). On the other hand the attenuation image (lower) shows the presence of the gas in the clay and the coarse sand with gravel as highly attenuated areas (yellow and red color). These results were confirmed by comparing with the boring log.

2.5 Advantage of the new method (3) "noise proof"

The conventional seismic tomography can't be conducted at a noisy place because the noise level becomes bigger than the amplitude of the propagated wave in the ground. This is a significant problem in an urban area where there are big background noises caused by lots of traffics and factories. But the new tomography isn't affected by these back ground noises because a frequency band of the new tomography is

Fig. 11. Photo of the filed data acquisition near by Tokyo Circuit Way No.7 which was one of the big roads which have a heavy traffic in Japan.

much higher than the background noise though the frequency band of the conventional tomography is almost same as the background noise as shown in Fig.10. The new tomography allows us to take data in the urban area such as near big road as shown in Fig.11.

The deference between the new tomography and the conventional tomography are listed summarily as shown in Table.2. It is clearly understood that the new tomography has the better resolution, more information and a shorter processing time though the survey area of these methods are the same.

3 PAST RESULTS

In this section, we explain two past results to clarify the advantage of the new tomography.

3.1 Pier extension work at Port of Manila

To extent the existing pier to offshore at Port of Manila at Manila Bay where has a big river, the pile foundation work had been conducted. Since a fluctuation of the bearing layer was found by boring log, this new tomography was conducted to investigate a bearing layer of the pile foundation because the boring log showed that the depth of the bearing layers were different between two boreholes as shown in Fig.12. Fig.13 shows the velocity image of the result at 2kHz in frequency and 50m in distance between two boreholes. From the boring log, the sand layer with gravel which was bearing layer was known to exist below a silt layer. In the velocity image, there were fast layers (red color) and slow layers (blue and green color). Comparing the velocity image with the boring logs and SPT results we understood that the fast layers meant the sand layers with gravel and the slow layers meant the clay layers. The upper boundary of the bearing layer is drawn as white dotted line in Fig.13. The numbers of the pile driving times per meter at each depth are also drawn as solid lines. A reasonable agreement between the depth where the numbers of the pile driving times increase suddenly and the upper boundary of the bearing layer are obtained. It was verified that the velocity image accurately represented the ground structures.

Table 2. Difference between the new tomography and the conventional tomography

Description	New method	Conventional method
Resolution (frequency)	-1m (1- kHz)	-5 m (-200Hz)
Survey Area	-100m	-100m
Results	Velocity Attenuation	Velocity
Processing time	1 hour - 1 day	2-3 days

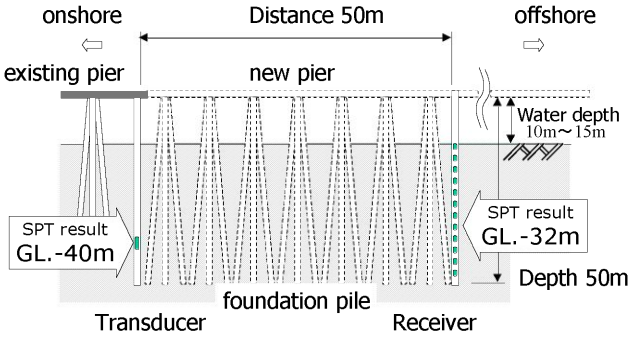

Fig. 12. Cross section of the pier extension work at Port of Manila. The transducer and the receiver were installed into the onshore side borehole and offshore side borehole respectively.

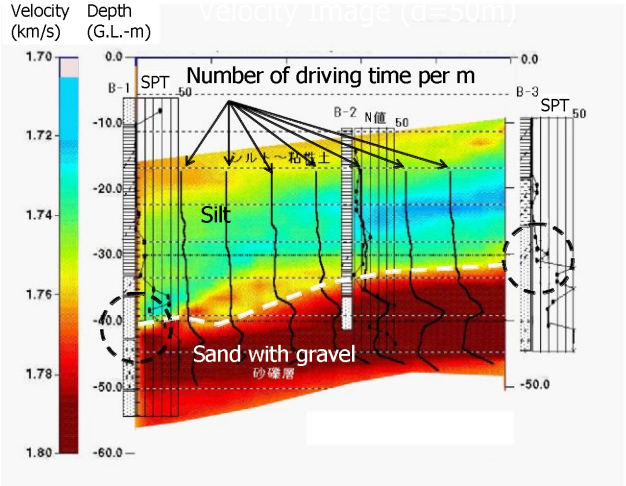

Fig. 13. Velocity image of Port of Manila at 2kHz in frequency, 50m in distance between two boreholes. White dotted line shows the upper boundary of the bearing layer and solid line shows number of pile driving time per m.

3.2 Multistory car park in Chubu International Airport

To build a multistory car park in Chubu

International Airport, two problems were encountered. First, piling work by driving a pile which made a big noise was prohibited because the airport was in operation. Second, the bearing layer which was a firm silt layer highly fluctuated. So a bored pile method had to be conducted at that time because of airport regulations. But by this construction method, it was quite difficult to adjust the pile length to the fluctuated bearing layer by cutting and pasting the pile, and 10 sections of the new tomography were conducted to obtain the accurate depth of the bearing layer. Fig. 14 and Fig.15 show the layout of the tomography measurement and the velocity image of Sec.7 respectively. The upper boundary of the bearing layer was drawn as solid line in Fig.15 by comparing with the boring logs and SPT results as same as Port of Manila. The velocity of the firm silt layer and the silt layer were 1.8km/s-1.9km/s (yellow and red) and 1.6km/s-1.7km/s (blue) respectively. To design the pile length accurately, a contour map of the depth of the bearing layer was made by putting all the velocity images together as shown in Fig.16. The complicated ground structure such as hollow, basin and steep and gentle slope were appeared. To verify the contour map of the depth of the bearing layer, the result were compared with the depth obtained from the drilling torque which increased at the firm silt layer as shown in Fig.17. The reasonable agreement between the contour map and the depth obtained from the drilling torque were confirmed.

To calculate a cost advantage of the new tomography, making a contour map obtained from only the boring logs as shown in Fig.18, designing the pile length and estimating its cost were done. Table.3 shows quantitative comparison between the design only by the boring log and by tomography. Table.4 shows cost comparison calculated by Table. 3. We found that the contractor was able to save his extra cost which was about 300 thousands US dollar. This was about 40 % of the total cost of the piling work.

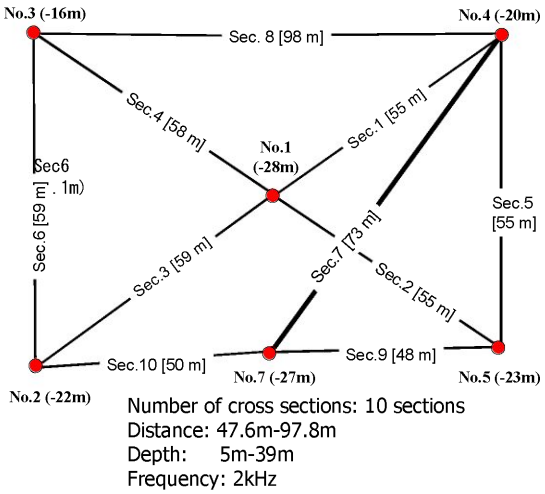

Fig. 14. Layout of the tomography measurements in Chubu International Airport

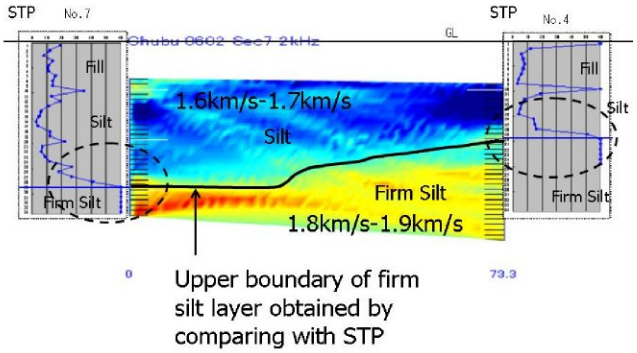

Fig. 15. Velocity image of Sec.7 at 2kHz in frequency, 73m in distance between two boreholes. Solid line shows the upper boundary of the bearing layer.

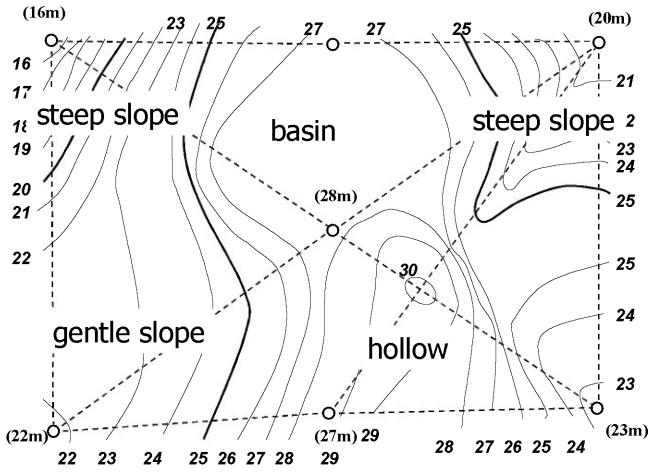

Fig. 16. Contour map of the depth of the bearing layer by putting all the velocity images together. Italic numbers show the bearing layer depth obtained from the velocity images, numbers in parentheses show the bearing layer depth obtained from the boring log.

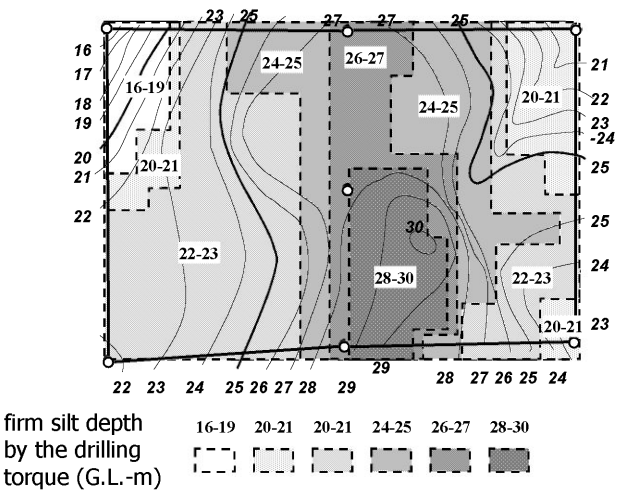

Fig. 17. Comparison between the contour map and the depth by the drilling torque (hatching and bolded numbers)

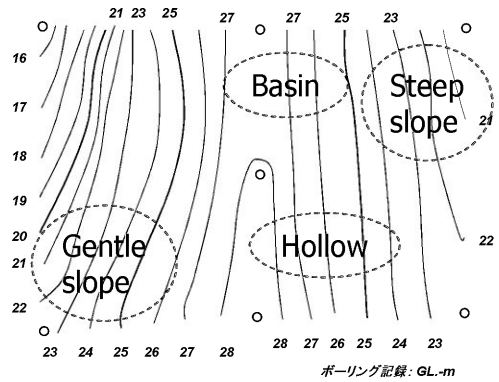

Fig.18. Contour map obtained from only the boring logs. Italic numbers show the depth of the bearing layer.

Table 3. Quantitative comparison between the design only by the boring log and by tomography

Designed by	Pile length (m)
Only boring log	6,177
Tomography	5,295
Difference	882

Table 4. Cost comparison calculated by Table. 3

Item	Amount	Price (U$)
Material	882 m	105,840
Equipment	882 m	79,380
Labor	211 piles	120,270
Total		305,490

.

4 CONCLUSION

The high frequency seismic tomography was explained by comparing with the conventional method. This new method is characterized by the high resolution, the long distance, the easy interpretation and the noise proof. Some geological survey methods were compared from points of the view of the survey distance and the resolution as shown in Fig.19. It is understood that the conventional methods are not able to satisfy "Useful resolution for design" and "Useful distance for cost" but the new method is able to satisfy both of these at the same time.

Finally a new construction flow by using the high frequency seismic tomography is proposed as shown in Fig.20. Conducting this new tomography before designing can provide a suitable design, a safety work and reducing cost and work period. On the other hand, safer designing only by the boring survey may bring over-design or extra order of materials. Moreover this may bring an increasing cost and work period caused by the trouble such as shortage or excess of the pile length.

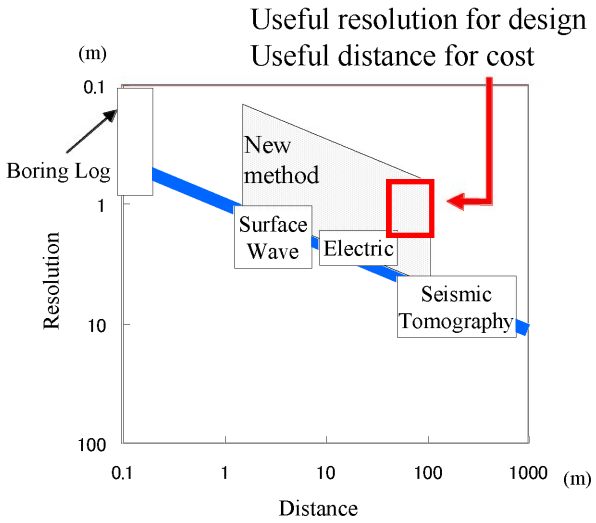

Fig. 19. Schematic diagram of comparison of geological survey methods from points of view of the survey distance and the resolution

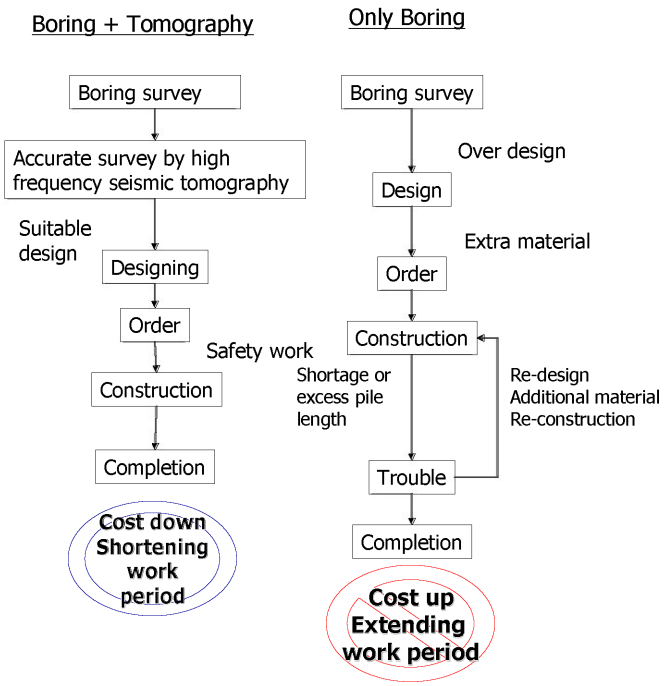

Fig.20. Flow chart of construction. Proposed flow by using the new method (left) and conventional flow (right)

Acknowledgement

We thank Mr.Toyokazu Skakaki, Tokuo Yamamoto for their helpful advising and discussion. We also thank Mr.Hisakazu Tajika, Mr.Kenichi Tomishige, Mr.Masato Tanaka and Mr.Masao Sugiyama for their helping us to take data in the field and to process the data. We also thank Chubu International Airport corporation for their accepting to publish the tomography results.

REFERENCES

1) Sakakibara, J. Yamamoto, T. (2009): Development of high-resolution geological survey by high frequency seismic wave, *Journal of Geotechnical Engineering*, Vol.65, No.1, 97-106 (in Japanese).
2) Yamamoto, T., Nye, T., Kuru, M. (1994): Porosity, permeability, shear strength: Crosswell tomography below an iron foundry, *Geophysics*, Vol.59, No.10, 1530-1541, 1994.
3) Bergman, N.D., Bailey, R.C., Chapman, C.H. (1989): Crosshole seismic tomography, Geophysics, Vol.54, No.2, pp.200-215.
4) Cunningham, A.B. (1979): Some alternate vibrator signals, Geophysics, Vol.44, pp.1901-1921.